LA-UR-13-27712
Approved for public release; distribution is unlimited.

Title: Summaries of FY13 LANL experimental campaigns at the OMEGA Laser Facility

Author(s): Loomis, Eric Nicholas

Intended for: Laboratory for Laser Energetics Annual Report
Report

Issued: 2013-10-03

Summaries of FY13 LANL experimental campaigns at the OMEGA Laser Facility

Overview

In FY 2013, Los Alamos National Laboratory (LANL) executed 207 total shots on OMEGA. LANL experiments contributed to the National Ignition (NIC) campaign in the following ways:

- Measured the x-ray ablative Richtmyer-Meshkov growth of isolated defects on beryllium ablators
- Studied branching ratios and species separation (plasma kinetic effects) in DT fusion plasmas
- Continued neutron imaging and gamma ray scintillator development for NIF
- Studied the suppression of hohlraum LPI with magnetic fields

High-Energy-Density (HED) campaigns included:

- Studied shear in a counter-propagating flow geometry driving turbulent mixing
- Backlit defect implosion experiments to study polar direct drive symmetry control
- Measured spatial distribution of mix in gas-filled capsules
- Imaging x-ray Thomson scattering platform development for dense plasmas and warm dense matter equation of state
- Measurement of a supersonic radiation wave and foam aerogel EOS

Shear

In FY13 the Shear campaign focused on extending our counter-propagating flow platform for studying shear-driven turbulent mixing to include long duration streaked imaging of the mix layer. These experiments used beryllium tubes containing low-density polystyrene foam half-cylinders separated by aluminum tracer layers. The counter-propagating flow is created by inserting gold "plugs" in front of each foam semi-cylinder at opposite ends to hold back the shock in each foam at one end (see Fig. xxx). With the plugs in place the beryllium tube ends are irradiated with 10^{15} W/cm^2 laser intensity to initiate counter-propagating shocks. When the shocks cross they establish a shear layer in the aluminum, which then grows due to Kelvin-Helmoltz followed by turbulent mixing.

In our November FY13 shot day we switched from x-ray framing camera based radiography of the mix layer to a long duration streaked imager. This required designing an area backlighter that would emit x-rays over 5 ns or longer to be recorded with an OMEGA streak camera (SMP with 20x magnification). Thin scandium foils sandwiching a thicker beryllium foil allowed us to irradiate both sides of the backlighter with grouped beams staggered in time. The central beryllium foil prevented burn thru, but still allowed significant transmission of x-

rays from the back scandium foil. An example streaked image is shown in Fig. xxx where the laser turn-on is indicated along with the mix layer (aluminum tracer foil), which shows the absence of signal due to x-ray absorption in the aluminum. The summary of mix width data is shown in Fig. xxx comparing simulations using the Los Alamos BHR turbulent mix model, streaked imaging, and x-ray framing camera data.

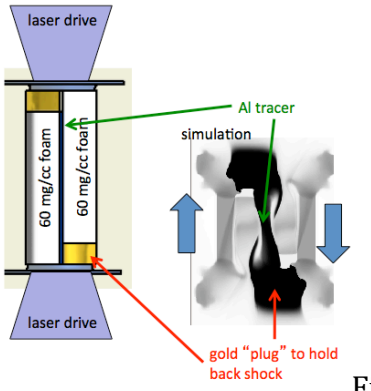

Fig. 1: Target geometry and simulated radiographs for counter-propagating shear experiments

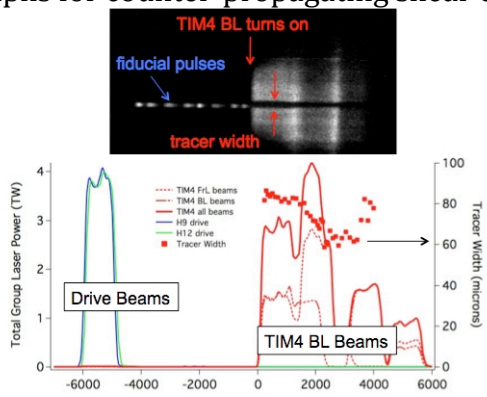

Fig. 2: Raw (top) and analyzed (bottom) streak data of mix width from shear experiments

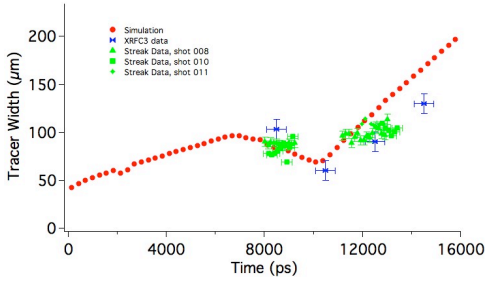

Fig. 3: Comparison between framing camera, streak camera, and simulated mix width evolution

BeARM

The Be ablative Richtmyer-Meshkov (BeARM) campaign had one shot day in January FY13. The overall goal of these experiments was to measure the oscillation

frequency of small perturbations on CH and Be ablators driven by the x-ray ablation Richtmyer-Meshkov effect. With this knowledge we would have a better understanding of how isolated defects behave during the first shock transit stage of a NIF ignition attempt, which could then provide methods for minimizing perturbations at the onset of Rayleigh-Taylor.

Our experiments used 15 beams inside large Au half-hohlraums, which were staggered in time to produce a 7.5 ns radiation drive with radiation temperature of 80 eV (see Fig. xxx). Targets with 2-D arrays of 5 micron tall, 17 micron FWHM Gaussian bumps and 25 micron wavelength Be sinusoids were attached over the opposite laser entrance hole with the defects facing inside the halfraum. During the experiment the bump arrays were backlit with Y and Ta backlighters (~2.2 keV emission) and imaged at 37x magnification onto an x-ray framing camera. Radiation hydrodynamics simulations running with Equation of State (EOS) tables for Be predict these small amplitude (2.5 micron) sinusoids undergo damped oscillations for our experimental conditions as shown in Fig. xxx. We measured the ablative RM of the Be sinusoids with 4 data points extending out to 7 ns as shown in Fig. xxx. At the two data points around 3.5 ns the sinusoids appeared to go through an inversion and then reappear by 7 ns. This appears to be consistent with the 20 micron simulation of Fig. xxx where the inversion occurs around 2 ns and then the inverted sinusoid reaches a minimum by 6 ns. With the slightly longer wavelength of our targets (25 microns) the inversion would be delayed slightly along with the time of the minimum of the inverted sinusoid.

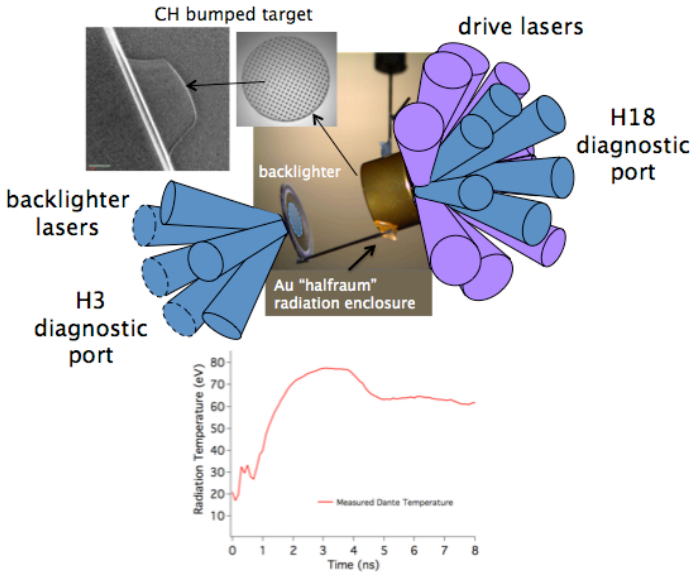

Fig. 4: Overview of indirect drive ablative Richtmyer-Meshkov experiments

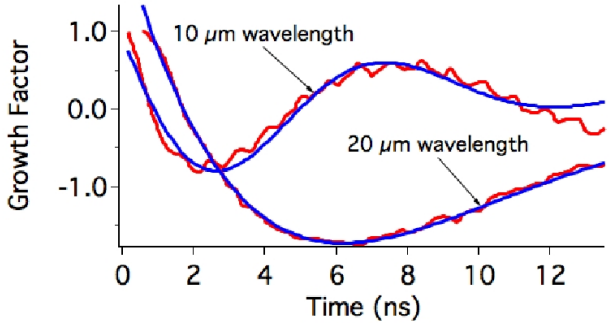

Fig. 5: Simulated oscillations of ablative RM sinusoids in Be

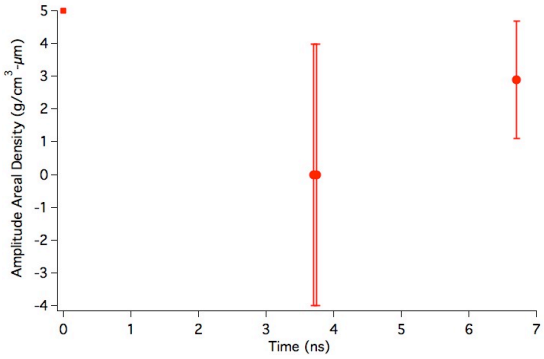

Fig. 6: Measured areal density of Be sinusoids. An apparent inversion is reached near 4 ns. The point at 7 ns is likely an inverted feature (local minimum), which was not apparent directly from the data.

GRH

The ICF gamma ray physics team, led by Hans Herrmann and Yongho Kim of P-24, completed 24 ICF implosions on Omega over 2 days (Sept 4, 5) investigating Plasma Kinetic Effects and Turbulent Mix. Plastic capsules of 4 different shell thicknesses were shot at 2 different fill pressures for each thickness in order to vary the ion temperature and density, and hence the ion mean free path. Performance predictions were provided by Nels Hoffman and Mark Schmitt, of XCP-6, prior to the shot day. Nels is in the process of developing a reduced ion-kinetic transport model for fluid simulations of high-Knudsen-number capsule implosions, where the Knudsen number is simply the ratio of the thermal-ion mean free path to the characteristic system dimension (i.e., approximately the distance from the center of the compressed core to the cold shell). The plasma kinetic terms of ion diffusion, viscosity, and thermal conduction (i.e., conservation of mass, momentum and energy) as well as reactivity reduction by free-streaming ion loss near the Gamow peak are incorporated into the reduced model. Turbulent mix is also allowed to play a role, although it did not appear to be a dominant factor in these implosions. An extensive suite of diagnostics was employed to enable the most highly constrained simulations to date. Measured attributes include laser energy coupling, DT & DD neutron yields and ion temperatures, fusion reaction histories, x-ray imaging and areal densities of fuel and shell. Preliminary experimental results in terms of yield and ion temperature are

reasonably close to predictions from the new model, as seen in the figure, but there are some remaining discrepancies (by comparison, yield-over-clean was typically in the 5-25% range). In particular, simulations tended to slightly over-predict yields at low ion temperature (while remaining within the uncertainty of the prediction), and under-predict at high ion temperature for the 5 atm fills. Notably, the ~7 um thick capsules at 2 atm fill pressure did not achieve the high predicted ion temperatures (~12 vs 16 keV), but yet still achieved the predicted yields. Detailed experimental analysis and post shot simulations accounting for "as-shot" parameters are in progress.

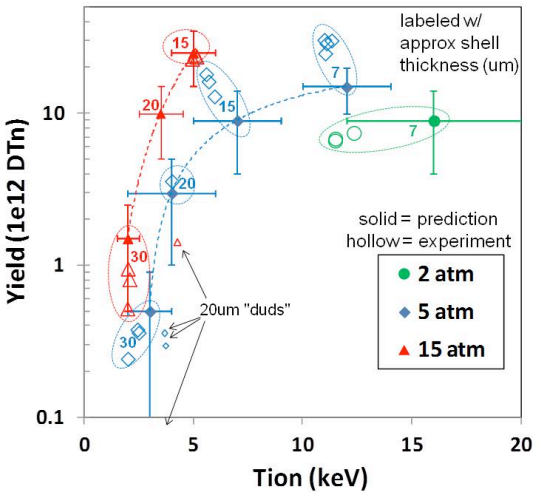

HED-MMI

Spatially resolving mix brings with it difficulties in interpretation

An exciting possibility to measure spatial information about the mixing has been doping of the inner wall of plastic shell in conjunction with a relatively new diagnostic allowing spectroscopic imaging of the atomic emission. The spectroscopic imager, termed a multiple-monochromatic-imager (MMI), consists of a pinhole array in front of an x-ray crystal. This produces many dispersed images that can be parsed to provide images over a narrow bandwidth. Alternatively, one may obtain the spectrum emitted from particular zones of the image.

In June 2012 experiments at OMEGA laser facility in Rochester, LANL researchers Rahul Shah and John Benage (both of P-24) in collaboration with the University of Nevada-Reno group of Prof. Roberto Mancini obtained images with the MMI imaging spectrometer of such doped targets. To be differentiated from experiments described below, these targets were doped uniformly around the entirety of the spherical shell. As small-scale features were expected to dominate the mix and create symmetric annular emission, the team was surprised, to instead find strongly asymmetric images. Most importantly, the features cast doubt on the ability to interpret if dopant emission was from central regions or localized along the shell-fuel interface as predicted.

Specialized targets provide insight into spatial features of the mixing

To address the difficulty in interpretation, the researchers worked with target fabrication teams at both LANL (MST) and General Atomics. As a result of this collaborative effort, targets were fabricated in which only a small patch of the capsule shell was doped. Such a localized doping along the equator of the implosion coupled with imaging down the capsule pole could avoid obfuscation of interior information by surface emission. In February of this year, Shah and Benage, along with a student from the university collaboration returned to Rochester to test this approach and its relevance to the long standing absence of images revealing just how deeply shell mixes into the imploding cavity. Fig. 1 shows images obtained at the Heβ emission line with such a target using two separate spectral imagers. The two instruments were operated simultaneously and on the same shot, but oriented so as to provide different views (as illustrated in the insets). In Fig. 1(a) the quasi-polar view very clearly shows that the brightest emission, which in the previous experiment could not be clearly identified as interior or surface, remains near the outside of the capsule. One also notes signal –originating from the dopant which initially was in the shell - is present across the image. The more face-on view of Fig. 1(b) evidences substantial transverse migration of the dopant.

Figure 1: Images obtained with modified targets with localized doping of shell. Spectral images formed at He-β emission line of dopant for both (a) quasi-polar and (b) quasi face-on views. Images were obtained using two separate MMI instruments operating simultaneously on same shot. Diagrams in each sub-figure show orientation of patch.

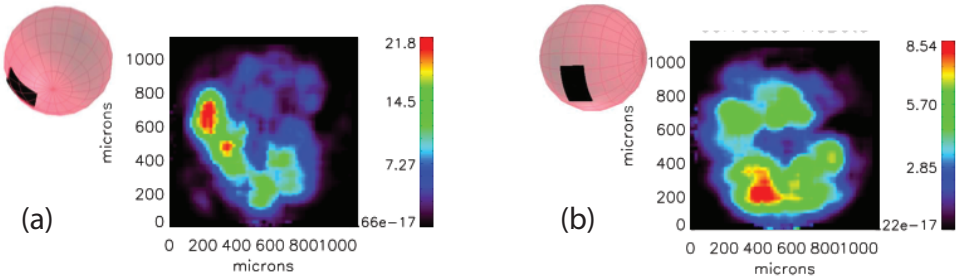

DIME

For the January 2013 Defect-Induced Mix Experiment (DIME) on Omega, the primary objective was to demonstrate the ability to manipulate spherical implosion symmetry with 40 beams in the polar direct-drive (PDD) configuration. Typically, with equal-power PDD beams and preferred LLE pointing, our capsules compressed with an oblate (pancake) configuration – a major/minor axis ratio increasing in time to > 2:1. For the January campaign, we explored two modifications of PDD: 1) We changed the energy balance for the three sets of PDD beam cones as a function of polar angle, $E(\theta)$. We reduced the nominal

polar cone power and increased equatorial power to mitigate the oblate effect. As we cooled the poles and provided enhanced heating to the equator, models and experiments showed a capsule transformation away from the oblate shape (Fig. 1). 2) A change in beam pointing was conducted on the second shot day with a second $E(\theta)$ scan. As predicted by simulations, the second-order Legendre mode P_2 was reduced (Fig. 2), but a fourth-order mode P_4 left the capsules with a 'rounded diamond'-like shape. Still, this campaign proved that control of independent PPD-cone power and pointing can impact capsule symmetry.

DIME: cone energy variation with the usual pointings, 850-μm CH capsule, 17 thick

Shot #	Cone Beam Energy (J)	Neutron Yield	Ti (keV)	Bang time (ns)	P_2 (exp)	P_2 (Sim)
68467	400/400/400	1.51E+10	3.25	1.85	-11.1%	-16.6%
68469	333/400/433	2.45E+10	3.66	1.88	-3.6%	-8.0%

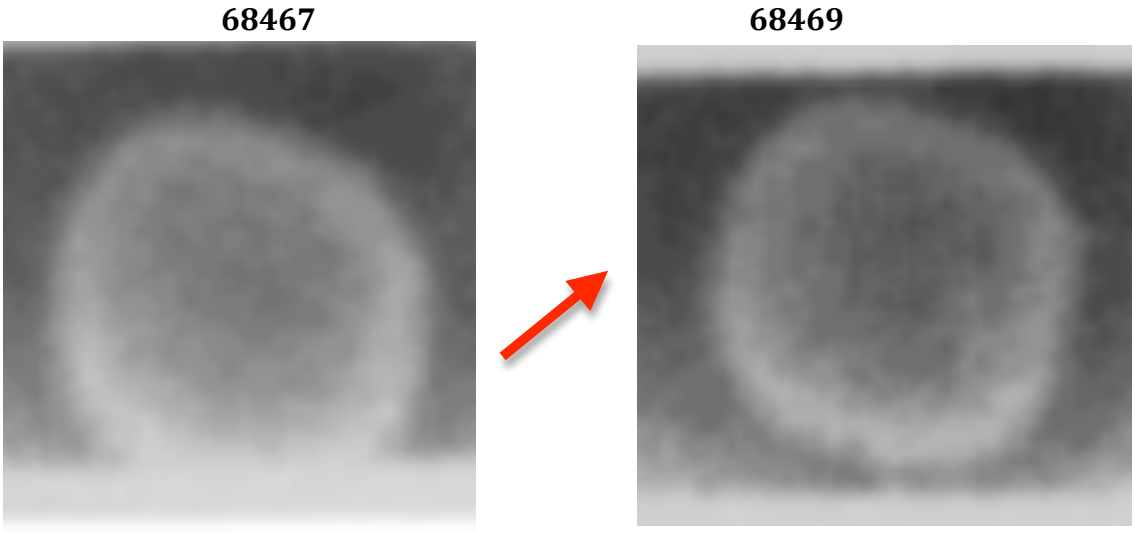

Figure 1. Images taken at time when R~0.5 R_0 Direction of the pole as indicated.

DIME: cone energy variation with new pointings, similar capsules

Shot #	Cone Beam Energy (J)	Neutron Yield	Ti (keV)	Bang time (ns)	P_2 (exp)	P_2 (Sim)
68486	333/400/433	1.28E+10	3.08	1.88	-7.5%	-6.1%
68489	400/400/400	2.01E+10	3.57	1.87	-3.1%	-7.5%

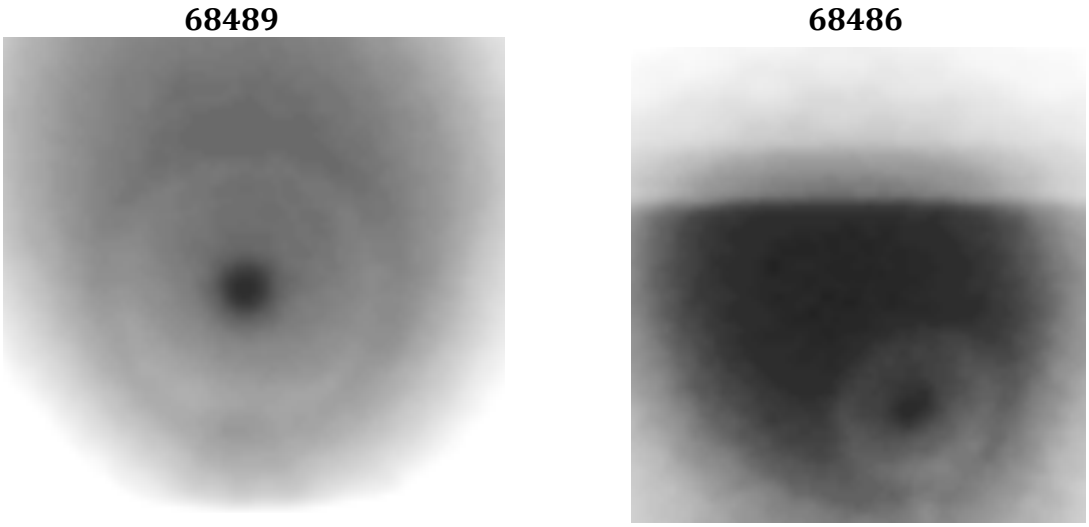

Figure 2. Image taken at time when R~0.6 R_0 Image taken at time when R~0.4 R_0

DPEOS

The major goal for the DPEOS project on Omega was to successfully obtain a complete set of equation of state (EOS) measurements on Carbon. The technique we are using, laser driven shock and release combined with imaging x-ray Thomson scattering, should enable us to obtain, for the first time, measurements of density, temperature, and pressure for materials at warm dense matter (WDM) conditions. To this end, two experimental days were carried out in FY13. The first on December 13, 2012 where we obtained 13 shots and a near 100% data return and the second on May 29, 2013 where we completed 15 shots and also obtained a very high data return rate. The emphasis on the first day was to obtain x-ray radiographs for our targets along with improving the Thomson scattering measurements. The results from that shot day indicated that the warm dense matter conditions in the target were being produced too long after the laser drive was off, negating the effectiveness of the pressure measurement. The experimental target and laser drives were reconfigured for the second experimental day with a dramatic improvement in the results.

Our results for the second day have been analyzed and we now state with confidence that we have demonstrated this technique can be used to obtain accurate measurements of density, temperature, and pressure for materials in the WDM regime. An example of our Thomson scattering results is shown in figure 1. Here we show our analyzed scattering results from shot 69918 and fits to these results at various temperatures. This data, combined with

results from the x-ray radiography and the VISAR and SOP measurements, have been used to determine density, temperature, and pressure for Carbon at three distinct conditions. We find that our results compare favorably to quantum molecular dynamics (QMD) calculations at these conditions. This is shown in figure 2 below where the data is compared to QMD and several SESAME EOS models. There is also reasonable agreement with several EOS models for Carbon, though some models compare better than others.

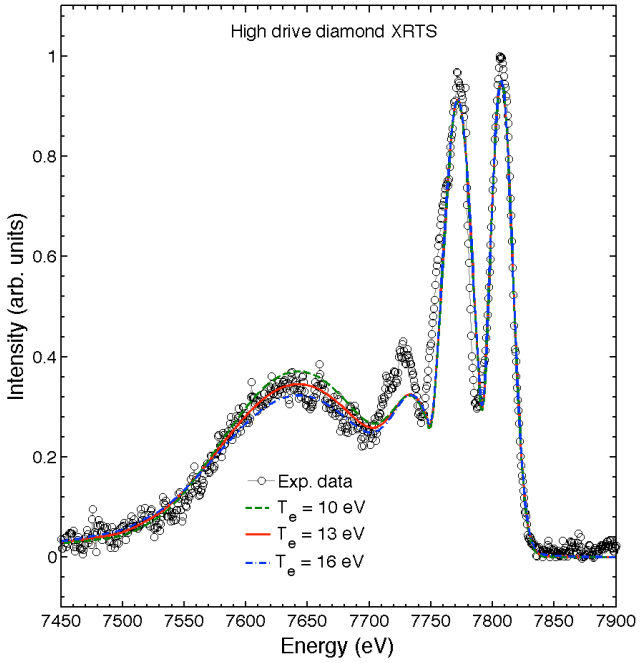

Figure 1. X-ray Thomson scattering data analyzed from Omega shot 69918. The fits to the data are utilize the known x-ray source spectrum from the Ni backlighter, the scattering angle of 100 degrees, and the density of 2.3 g/cm^3 obtained from the radiograph of this shot.

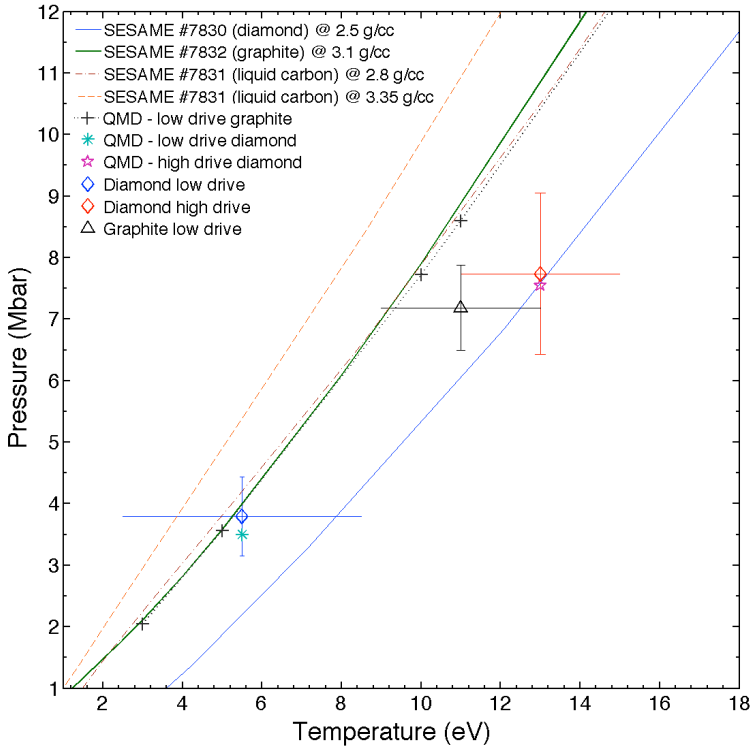

Figure 2. Comparison of WDM carbon measurements to various isochors of EOS models of carbon. The data points (marked by inclusion of error bars) represent carbon at 2.8 g/cm^3 and 5.5 eV, 3.1 g/cm^3 and 11 eV, and 2.3 g/cm^3 and 13 eV. The corresponding QMD calculations are color matched and compare very well with the data except for the 11 eV point. For this case we have plotted the QMD results for 3.0 g/cm^3 and several temperatures and we see that these fall within the uncertainty of the measurements.

NIF5

The major goal for the NIF5 project on Omega was to successfully obtain temperature measurements from shocked aerogel foams and shocked CH foams using the SOP diagnostic. To accomplish this goal, two experimental days were carried out in FY13. The first on November 7, 2012 where we obtained 15 shots and a high rate of data return and the second on May 1, 2013 where we also completed 15 shots and obtained a high data return rate. The emphasis on the first day was to obtain temperature data from our aerogel foam targets at a range of conditions. The second experimental day focused on the CH foams, which had an initial density of 0.15 g/cm^3.

The results for the two days indicate two important things. First, the temperatures measured for the silicon aerogel foams agree with EOS models at low pressures, but drop below the models as the pressure is increased. We also find that it is below temperature values obtained using QMD

calculations, which we expect to be quite accurate at these low temperatures. This is shown by the graph below in figure 1. We are presently doing highly resolved simulations of the shock process to better understand the physics mechanisms behind this difference. Similar experiments on CH were done on the second day. The results were a little surprising as the effective temperatures were quite a bit lower than the aerogel temperatures for a given pressure drive. This is likely because of the higher bond and ionization energies for CH. Further data analysis is ongoing.

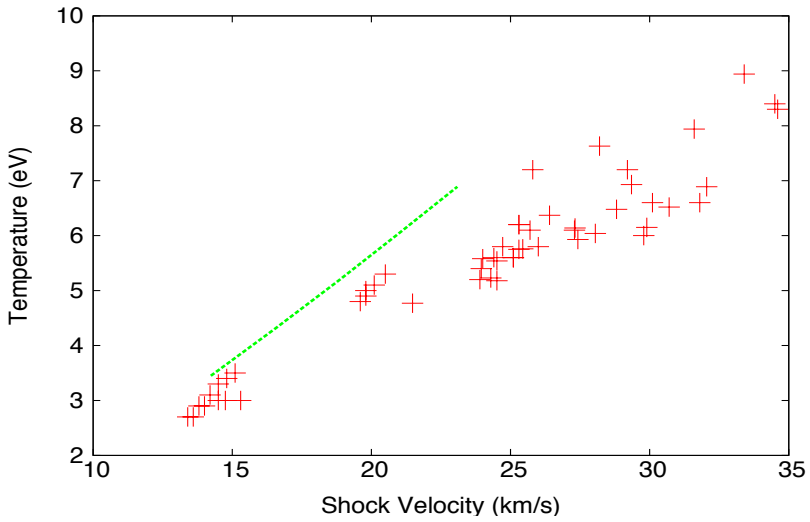

Figure 1. SOP temperature measurements for shocked aerogel foam. The red crosses represent individual data points and the green curve is from QMD calculations for the EOS of the shocked foam.

MagLPI

The goal of the MagLPI campaign on the Omega Laser Facility is to demonstrate laser-plasma instability (LPI) mitigation using magnetic fields. Using a sufficiently strong external magnetic field, thermal heat transport is expected to be reduced across a magnetic field since the transport step-size is determined by the electron Larmor radius instead of the electron-ion collisional mean-free-path. In this regime of "magnetic insulation", the plasma electron temperature is expected to increase compared to the case with no external field. The ability to increase the underdense plasma temperature in a NIF ignition hohlraum is highly desirable since it would reduce inverse bremsstrahlung losses of the NIF inner beams as they propagate through the long scale length low-Z plasma. In addition, increasing the plasma temperature would significantly increase Landau damping and help mitigate stimulated Raman scattering (SRS).
Using a MIFEDS pulsed magnetic coil, an external field up to B_z = 8-T was applied with the field aligned along the axis of a gas-filled hohlraum at the Omega laser. The hohlraum axis was aligned along the P9-P4 ports, and 39 beams irradiated the

hohlraum in 3 beam cones. The 4ω Thomson scattering beam probed the plasma at the center of the hohlraum, as viewed through a diagnostic hole at the hohlraum midplane. The specific deliverables for this campaign were to measure the electron temperature, SRS backscatter and hard x-rays versus B-field strength.
A total of nine target shots were performed on August 20th, 2013. Preliminary results indicate an increase in plasma temperature with external B-field, and the correlation with LPI and B-field strength is currently being analyzed.

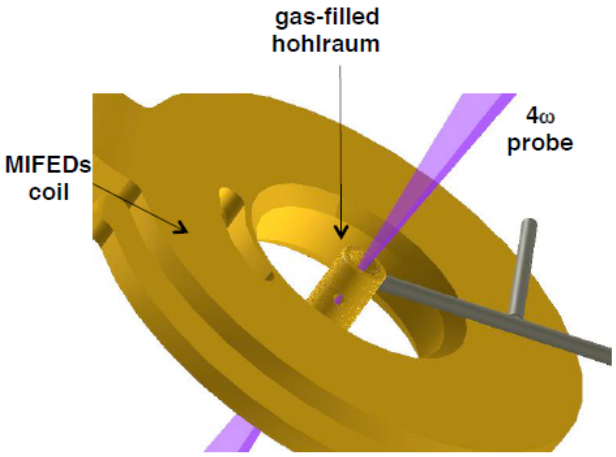

Figure 1: Schematic of experimental layout with MIFEDS coil, which generates an external magnetic field, and the hohlraum axis aligned along the 4ω Thomson probe beam axis.

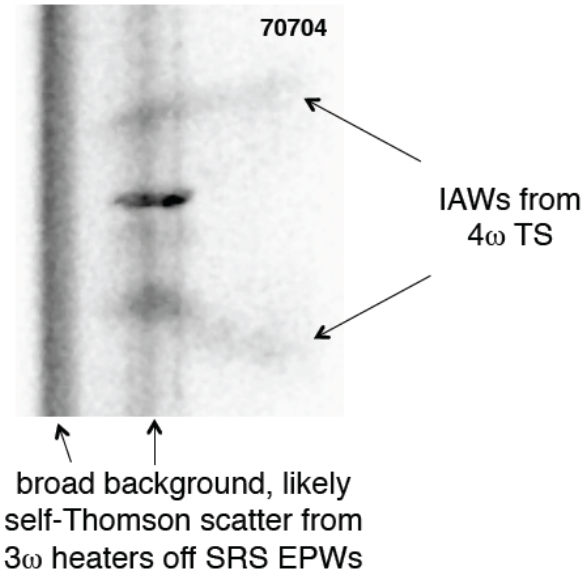

Figure 2: Thomson scattering measurement from thermal levels of ion acoustic waves (IAWs). Wavelength is in the vertical axis, and time is increasing to the right.

The separation between the IAWs increases with increasing plasma temperature.

Gamma Ray Imaging

On Tue. 6 Aug. 2013, Los Alamos National Laboratory successfully executed a full day of shots at the Omega Laser, Laboratory for Laser Energetics, University of Rochester, Rochester, NY in support of two experimental science campaigns. Characterization data of a novel Gamma Ray Imaging camera were collected, as well as hard X-ray aperture images of bremsstrahlung radiation produced by hot electrons traversing the remnant shell material from implosions of plastic capsules. The Gamma Ray Imaging diagnostic is being developed by LANL in collaboration the University of Arizona's Center for Gamma Ray Imaging. Further, LANL collected data in support of its Turbulent MIX DR project, shooting a variety of separated reactant targets, comprised of ^{3}He filled plastic capsules constructed with 1 um thick deuterated layers within the inner regions of the CH shell. In these experiments the fusion of d-^{3}He fusion reactions are used as the direct signature for atomic mix. Good neutron and proton yield data were collected, as well as gamma images of the implosions, as illustrated in the figure below.

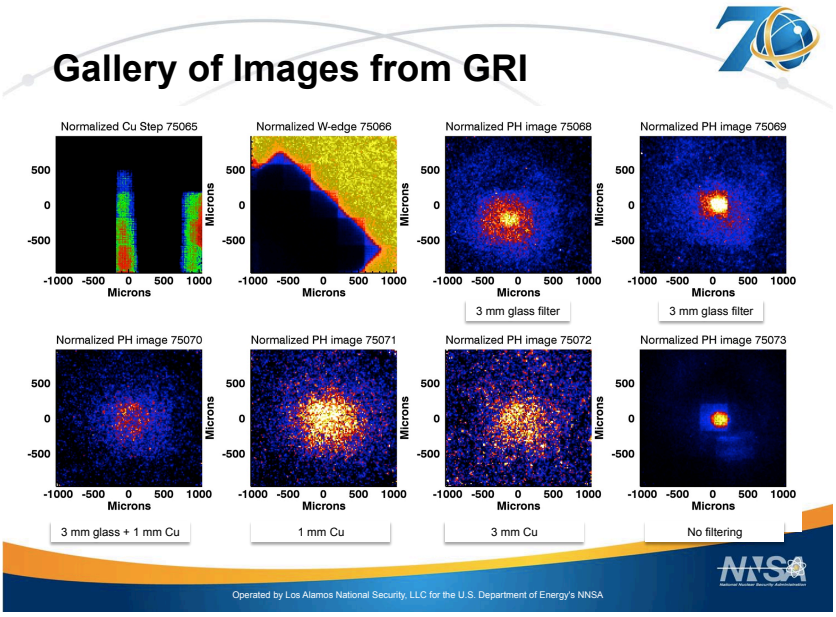

Neutron Imaging System

Imaging technologies are typically benchmarked with a known system to determine the residual distortions. In radiography a standard static object is radiographed, the analysis techniques are applied and the result of this analysis is compared to the

known object. This allows one to characterize the performance of the image formation and reconstruction algorithms. One of the difficult aspects of neutron imaging has been that no "standard" neutron source is available to perform this type of test. This has resulted in a strong reliance on modeling and simulation to characterize the performance of the image formation and reconstruction algorithms. No neutron source is suitable because the system is designed to image sources, which are very bright ($\sim 10^{17}$ neutrons/cm^2 at the source surface) and very small ($\sim$100 μm in diameter). The system was designed and tested through measurements at Omega, but these dynamic sources are not well enough characterized and reproducible to be used as a "standard" neutron source for bench marking the full system performance.

A series of experiments have been performed at Omega in the last year to overcome this limitation. In the design of these experiments simulations were used to determine the neutron flux at the detector, which results from a known neutron source after passing through the aperture array. A copper object was designed to generate this same neutron flux at the image plane when located just in front of the image collection system. These known static objects were then placed in front of the image collection system at Omega and the neutron flux passing through these objects were measured. The standard analysis techniques were used to extract the source information from these images, and this was compared to the simulated neutron source. This experimental data has allowed us to determine the system performance, including the detector and reconstruction algorithms. This data set allows us to partially overcome the limitation of not having a "standard" neutron source for benchmarking our detection and reconstruction algorithms.

Figure 1 shows the two images collected from two test objects. The left image shows the neutron flux after passing through an object designed to simulate a point source of neutrons while the right image shows the flux from a 20 μm diameter

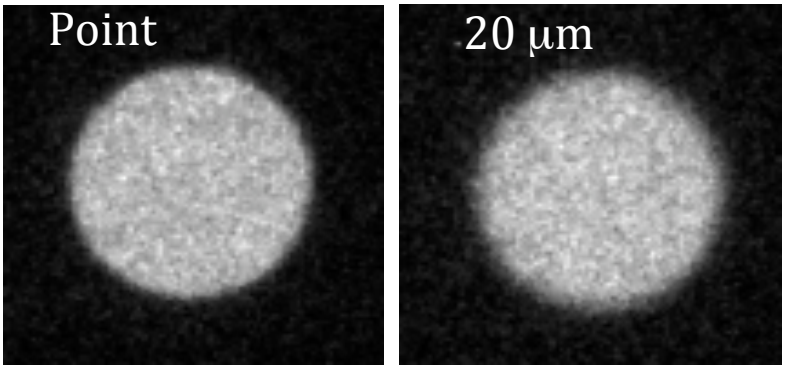

neutron source. These test objects were designed to generate the neutron flux that would be expected from the NIF geometry through the mini-penumbra presently being used at NIF.

Figure 1: Left, mini-penumbral image expected from a point source of neutrons through the NIF mini-penumbra. Right, mini-penumbral image expected from a neutron source with a P0 of 20 μm.

The standard set of reconstruction algorithms, which were developed for NIF data analysis, were used to process and reconstruct these images. The results are shown in figure 2.

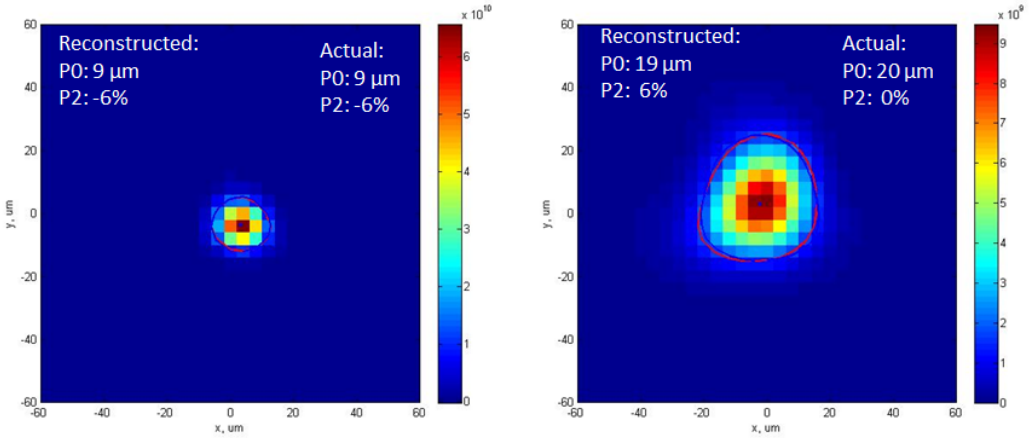

Figure 2: Reconstructions of the images shown above. Left, the point source reconstructed to have a radius or P0 of 9 μm and the source with 20 μm P0 resulted in a reconstructed P0 of 19 μm. The reconstruction of the point source provides a measure of the reconstructed resolution of this system. The good agreement between the actual and reconstructed P0 of the extended source demonstrates the performance of the reconstruction algorithms.

Over the past year a significant effort has been devoted to the determination of error bars in the reconstructed parameters. These estimates have come directly from simulations. However, one would expect that these measurements should be consistent with these error bars. To check this, simulations have been performed to determine the error bars in P0 and P2 for the extended source shown above to be ±1 μm ±5%, respectively. This is in good agreement with the observed reconstruction values.

These measurements have provided a test of our imaging system and analysis scheme using simulation through the aperture array combined with experimental measurements at each level. It has demonstrated the reconstructed resolution of the mini-penumbral apertures is ~10 μm and has provided confidence in our determination of error bars.

The DIME series of experiments, which are planned at NIF in the coming years, will rely on the neutron imaging system for a measure of the extent of mixing in the implosion of a separated reactant capsules. This requires the measurement and reconstruction of neutron source in the shape of a spherical shell. The thickness of this spherical shell provides a measure of the extent of mixing in these experiments. A series of measurements at Omega have been performed to test the mini-penumbral aperture that is being proposed for this measurement. A test object was constructed, similar to the objects described above, which can generate the flux of neutrons that is expected in these DIME experiments at NIF. These measurements were made to test the measurement and reconstruction methods to determine how well these mini-penumbra could be used to reconstruct a spherical shell neutron source. These measurements were collected in August, 2013 and therefore the

analysis is not complete, but the results are encouraging. Figure 3 shows the reconstruction of this neutron source, showing that the general characteristics of the spherical shell are recovered in these reconstructions.

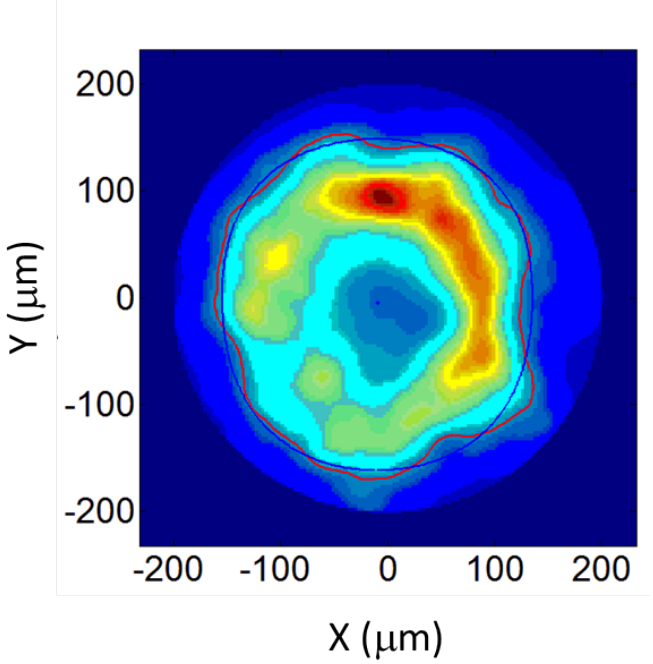

Figure 3: Reconstruction of the measured neutron flux from the test object that generates the flux of neutrons expected from the DIME experiments at NIF (150 μm radius with 50 μm width). This shows a clear spherical source. This data provides an opportunity for comparisons to simulation, ultimately characterizing the error bars associated with this type of measurement.

Neutron generating experiments at Omega continue to provide important data to fully characterize the neutron imaging system at NIF. These measurements provide a stringent test of our simulations and models as well as providing known sources for the testing of our reconstruction algorithms.